HOKKAIDO UNIVERSITY

Title	Parametric study on dynamic interaction of horizontally curved twin I-girder bridges and a moving vehicle
Author(s)	Awall, Robiul; Hayashikawa, Toshiro
Citation	Journal of Structural Engineering. A, 57A, 242-251 https://doi.org/10.11532/structcivil.57A.242
Issue Date	2011-03
Doc URL	https://hdl.handle.net/2115/67384
Type	journal article
File Information	Parametric study on dynamic interaction of horizontally curve.pdf



Hokkaido University Collection of Scholarly and Academic Papers : HUSCAP

Parametric study on dynamic interaction of horizontally curved twin I-girder bridges and a moving vehicle

Md. Robiul Awall * and Toshiro HAYASHIKAWA **

* Graduate Student, Graduate School of Eng., Hokkaido University, Kita 13 Nishi 8 Kita-ku, Sapporo 060-8628.
** Dr. of Eng., Professor, Graduate School of Eng., Hokkaido University, Kita 13 Nishi 8 Kita-ku, Sapporo 060-8628.

Behavior of horizontally curved I-girder bridges are complex and its interaction analysis is difficult. In this study, extended three-dimensional finite element interaction analyses were conducted parametrically. The bridge is modeled in detailed with solid and shell elements and vehicle is simulated as a nonlinear model according to HS20-44 design truck. Road roughness profiles are generated from power spectral density and cross spectral functions. By using these models, natural vibration and forced vibration analyses carried out in parametric study, are extensively investigated. The analytical results are significant and give some useful information regarding the impact factor of the studied bridge which could be much helpful for practical designer.

Key Words: Curved I-girder bridge; FEM; Interaction analysis; Impact factor

1. INTRODUCTION

Horizontally curved bridges are used vastly in modern highway interchanges systems because of increased demand for curved roadway alignments for the smooth passage of congested traffic and restraints of existing land use. Also, the modern emphasis on aesthetic considerations has motivated to increase the curved alignments uses. I-girder bridges are most preferred choice because of its simplicity of fabrication and construction, economy, erection technology, and serviceability performance. However, these I-girders have very little torsional stiffness and are stable only when connected to other girders using transverse members[1]. Due to the horizontal curvature, the bridge and its component members are subjected to coupled torsion and bending. For that reason the behavior of horizontally curved bridges are more complex and its analysis is more difficult than straight bridge. Bridge design codes usually provide for the dynamic effects in straight bridges, through some attention is paid to curved bridges where the curvature needs to be incorporated[2].

Comparatively little work has been undertaken in studying the curved bridges interaction dynamics compared to straight bridge. Senthilvasan et al.[2] studies the dynamic response of curved continuous box girder bridge by experimentally and finite element approach. In their study, they used simplified model of vehicle and initial vibration of vehicle and damping of bridge are not considered. Sennah and Kennedy[3] investigated the vibration characteristic of horizontally curved continuous bridge by experimentally and finite element approach with simplified moving concentrated load without considering surface roughness. Huang et al.[4,5] studies the interaction of horizontally curved I-girder bridge and box girder bridge respectively. Bridges were idealized as a planer grillage beam systems and the vehicle was modeled as a nonlinear model with 11 degree of freedom and interaction analyses are done numerically. Another analytical method of curved box girder bridge was developed by Samaan et al.[6]. They consider fairly smooth road surface and ignore super-elevation. Genin et al.[7] developed the algorithm by using Green functions to derive two coupled integral-differential equations governing the deflection and rotation of the curved bridge. For simplicity they modeled the vehicle as a mass resting on a parallel spring-dashpot suspension system. Another numerical approach was contributing by Mermertas[8]. His study is limited to vehicle speed and guideway parameters and vehicle is modeled as four degree of freedom with lumped masses, linear springs and dampers.

In these cited studies the interaction dynamics are treated as simple method and have some limitations because of geometric complexities of curved bridges. However, almost all of the analyses are local developed computer programs that were intended primarily for research use. Therefore, most practical

bridge engineers have limited benefit. Some previous studies utilized completely a commercially available computer codes for straight bridge interaction analysis, like Kwasniewski et al.[9] used LS-DYNA code and Martin et al.[10] used ANSYS code. However, no road surface roughness was taken into account and simple moving loads instead of moving spring-mass-dampers were considered in their study. Therefore it is important to extend the study on curved bridge-vehicle interaction dynamics and take into account for the dynamic amplifications in responses.

In this study, extended three-dimensional finite element models of horizontally curved twin I-girder bridges and AASHTO HS20-44 vehicle model are developed by using commercially available ANSYS code. Super-elevation is incorporated into the bridge model. By using the bridge-vehicle models dynamic interaction analyses are carried out parametrically to analyze their impact characteristics for the practical design and further impact studies of curved I-girder bridges with considering different parameters.

2. ANALYTICAL MODELS

Commercially available ANSYS Parametric Design Language (APDL) code was chosen to develop three-dimensional finite element models of studied bridges and vehicle. This code provides a vast capability for both static and dynamic analyses especially an advanced contact technology.

2.1 Twin I-girder bridge model

The original bridge chosen in this study is a simply supported horizontally curved twin I-girder bridge, whose length is 50m measured the centre line between two main girders. The two main I-girders are 3m deep and spaced transversely at 6m. These main structural members are tied together by a reinforced concrete slab which acts compositely with the girders and 11 equally spaced transverse cross beams. Original studied bridge geometric properties and cross-section layout are presented in Table 1 and Fig.1, respectively. The same cross sectional properties but several radius of bridges, namely R = 100m, 200m, 400m and 800m, measured from the origin of the circular arc to the centerline of the bridge deck are considered to take into account the effects of curvature. Because the length of the centerline is fixed, the average mass per unit length of the bridges and the cross sectional area are considered to be uniform. Super-elevation is considered in to the bridge model. AASHTO[11] suggest the maximum super-elevation rate for urban areas is 6% of the width of the bridge. Due to parametric analysis of this study three different super-elevation, namely e = 1%, 3% and 6% are considered.

Bridge structures can be modeled in many different ways. Here, bridges are discretized as three dimensional finite element models by using ANSYS code to analyze the interaction problems. The bridge is modeled in detail with hexagonal 8-node

Table 1 Geometric properties of studied bridge

Span length [m]	50
Deck width × thickness [m]	10.5 × 0.3
Dimensions of main girders [mm]	WEB 3000 × 24
	Upper FLG 500 × 30
	Lower FLG 500 × 50
Dimensions of intermediate cross-beams [mm]	WEB 1000 × 16
	FLG 300 × 25
Dimensions of end cross-beams [mm]	WEB 3000 × 16
	FLG 300 × 25

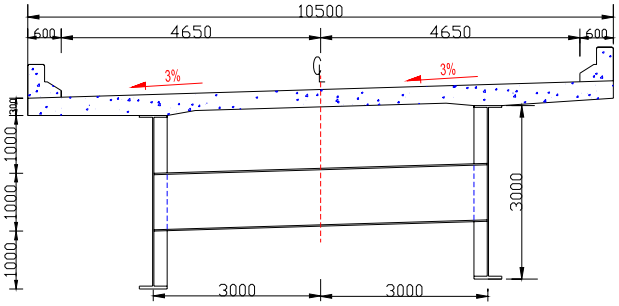


Fig.1 Cross-section of studied bridge (mm)

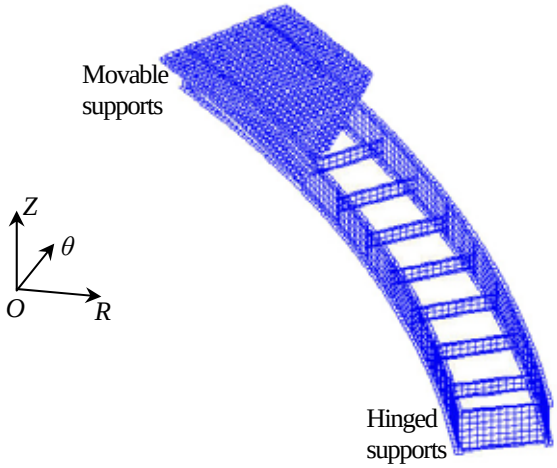


Fig.2 Detailed FE model of studied bridge (R = 100m & e= 3%)

Table 2 Boundary conditions

Type	u_1	u_2	u_3	θ_1	θ_2	θ_3
Hinged	*Fix*	*Fix*	*Fix*	*Free*	*Free*	*Free*
Movable	*Fix*	*Free*	*Fix*	*Free*	*Free*	*Free*

u_1, u_2, u_3 are translations in the R, θ, Z directions.
θ_1, θ_2, θ_3 are rotations about R, θ Z directions.

solid elements for concrete deck and quadrilateral 4-node shell elements with 6 degree of freedom at each node for all steel members. Both elements have large deflection capability to do the nonlinear analysis. All elements are defined based on cylindrical coordinate system whose origin is center of bridge's curvature. The typical finite element model of 100m radius studied bridge is shown in Fig.2. The boundary conditions at the end of the main girders are hinged and roller supports as described on Table 2. The roller support was modeled by

releasing the horizontal movement at tangential direction. However, the hinged support was constrained from any horizontal movement. All supports were constrained in vertical direction, but allowed to rotate around the support line.

2.2 Vehicle model

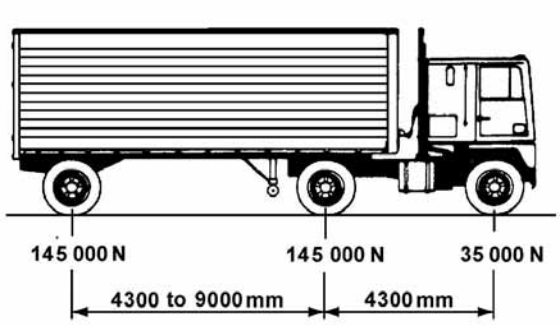
To conduct parametric study, standard HL-93 truck load model is used in conjunction with AASHTO LRFD2004 design truck HS20-44 and design lane load[12]. This type of vehicle is a major design vehicle in AASHTO specifications which is used by many researchers[4,5,6]. Weights and spacing of axles for the HS20-44 design truck and its finite element model are shown in Fig.3. The design truck is idealized as 3D nonlinear finite element model consisting of masses connected by rigid beams and supported by spring-dampers as shown in Fig.3b. The model consists of three dimensional five lumped masses with rotary inertias; represent tractor, semi-trailer and three wheel/axle sets. The upper spring-dampers represent the suspensions of the vehicle and the lower ones are for tires. Gap elements are incorporated to the lower spring-damper elements to imitate the separation between tires and road surface. Detailed model of this vehicle is found in a report of Ngo-Tran et al.[13]. Suspension force consists of the linear elastic spring force. The tire springs and all dampers are assumed to be linear. Principle stiffness coefficients of truck model are given in Table 3, these coefficients and others properties of masses and spring-dampers can be found in a report of Wang and Huang[14]. The vehicle is supposed to move at constant speed on a circumferential path along the bridge deck. It can be seen that the vehicle model is capable to take into account the effects of pitching, rolling, and bouncing of vehicle body as well as the effect of separations between tires and road surface.

2.3 Road profile model

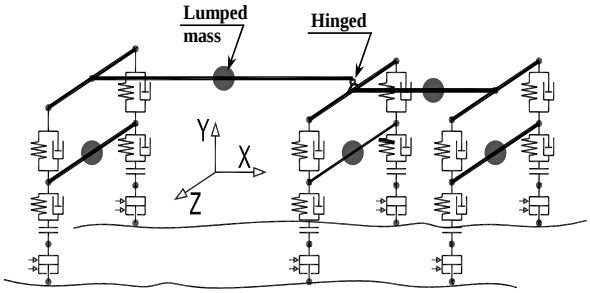
The bridge deck surface roughness is an important factor which affects the dynamic responses of bridge-vehicle system. In this study, road surface profiles are assumed to be periodically modulated random processes that can be described by Power Spectral Density (PSD) function proposed by Doods et al.[15] and Honda et al.[16] as in Eq. (1).

$$S(n) = S(n_0)\left(\frac{n}{n_0}\right)^{-w} \qquad (1)$$

Where, $S(n)$ = PSD (m^2/cycle/m); $S(n_0)$ = roughness coefficient (m^2/cycle/m); w = roughness component varied from 1.36 to 2.28; n = wave number (cycle/m); n_0 = discontinuity frequency = 1/(2π) (cycle/m). According to the Motor Industry Research Association (MIRA)[15] road surface roughness can be classified in to various groups and the parameter values for each group are given in Table 4. Typical spectral densities of a principle road with various roughness conditions are graphically presented as in Fig.4. In this study, principal road conditions are considered and selected roughness coefficient values for very



a) Geometric configuration



b) Finite element model

Fig. 3 HS20-44 design truck

Table 3 Stiffness coefficients of design truck

Items	Front Axle (kN/cm)	Drive Axle (kN/cm)	Trailer Axle (kN/cm)
Tire	8.75	35.03	35.07
Suspension spring	2.43	19.03	19.69

Table 4 Classification of roads based on road spectra[15]

Road class		$S(n_0)$ range (10^{-6})	w $n \le n_0$	w $n > n_0$
Motorways	Very good	2-8	1.945	1.360
	Good	8-32		
Principal roads	Very good	2-8	2.050	1.440
	Good	8-32		
	Average	32-128		
	Poor	128-512		
Minor roads	Average	32-128	2.280	1.428
	Poor	128-512		
	Very poor	512-2048		

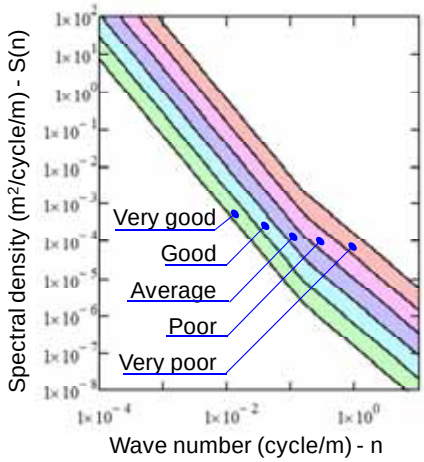


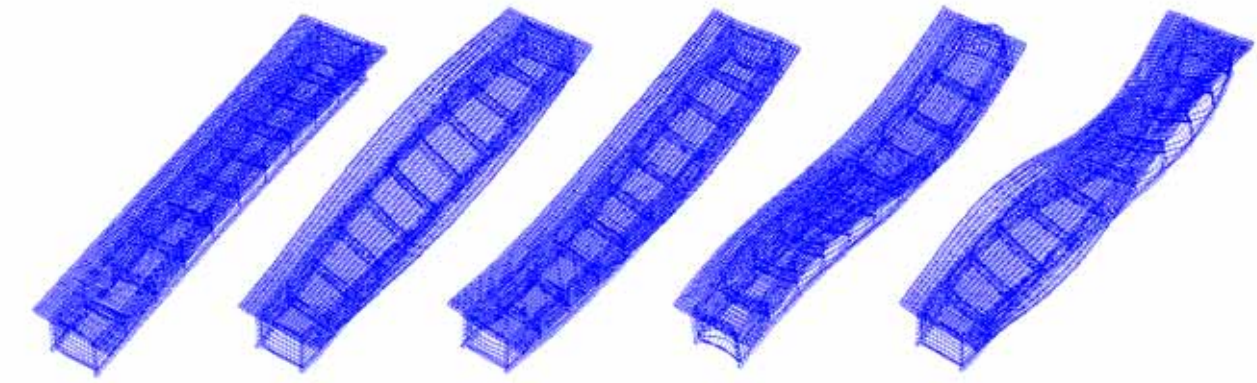
Fig.4 Spectral densities of a principle road

Table 5 Natural frequencies of studied vehicle

Mode	Frequency (Hz)	Nature of mode
First	1.47	2nd rear axle rolling
Second	1.79	Pitching
Third	2.06	Front axle bouncing
Fourth	2.21	Bouncing
Fifth	4.02	Front & 1st rear axle rolling

Table 6 Super-elevation effect on first vertical mode (V1)

	Frequency (Hz) of different super-elevation			
Radius	0%	1%	3%	6%
800	2.300	2.297	2.295	2.290
400	2.236	2.233	2.234	2.234
200	2.050	2.043	2.047	2.052
100	1.637	1.622	1.624	1.628



f_1= 2.234 Hz (V1) f_2= 3.103 Hz (T1) f_3= 6.048 Hz (TH1) f_4= 7.645 Hz (V2) f_5= 8.965 Hz (T2)

Note: V1- First vertical; T1- First torsional; TH1- First combine torsional horizontal; V2- Second vertical; T2- Second torsional

Fig.5 Several mode shapes of the studied bridge (R = 400m and e = 3%)

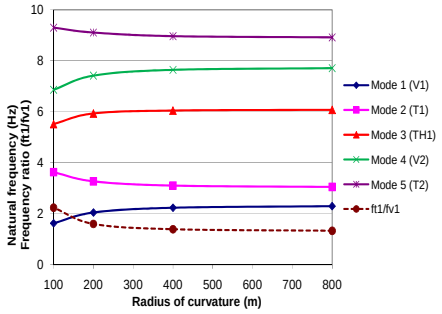
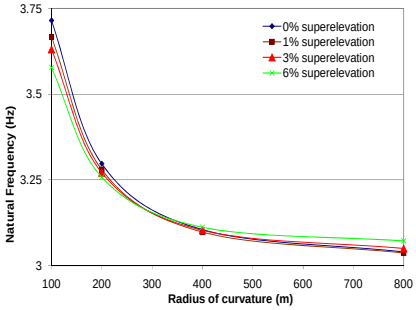
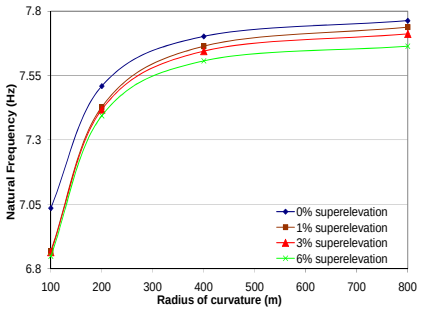


Fig.6 Natural frequency/frequency ratio with radius of curvature (e = 3%)



a) First torsional mode (T1)



b) Second vertical mode (V2)

Fig.7 Effect of super-elevation on 1st torsional mode (T1) and 2nd vertical mode (V2)

good, good, average and poor road surfaces are 5×10^{-6}, 20×10^{-6}, 80×10^{-6} and 320×10^{-6} respectively. Correlated road surface profiles are generated from PSD and cross spectral density functions by assuming road surface as homogeneous and isotropic random process[15,17]. Four types of road roughness profiles are generated for very good, good, average and poor roads. Details are founded in the reference of Ngo-Tran et al.[13].

2.4 Interaction between vehicle and bridge

To couple the motion of the vehicle and bridge structure, contact technology is employed in this study. ANSYS node-to-surface contact pair consisting of a target surface mapped on the surface of deck element and contact elements connected with actuator elements are adopted. This is the most widely used contact elements in ANSYS. This contact technique allows contact nodes to slide on the target surfaces with or without friction. Isotropic coulomb friction is considered to the analysis. Lagrange multipliers and kinetic constraint equations between these systems are utilized by using augmented Lagrangian method; which is an iterative series of penalty updates to find the Lagrange multipliers. This method is selected over others such as pure penalty, pure Lagrangian multiplier methods because it usually leads to better conditioning and is less sensitive to the magnitude of the contact stiffness coefficient while introduces no additional equations to the discrete system[18]. Correlated road surface roughness is input as stroke (length) of the actuator elements to simulate the unevenness of road surface.

3. ANALYTICAL RESULTS

3.1 Natural vibration analysis

The dynamic characteristics of a bridge, including its natural frequencies, vibration mode shapes are important factors which can significantly affect its stability behavior under traffic load. Natural vibration analysis results are investigated of different radii of bridges and different percentages of super-elevation of studied

bridges. Also, natural vibration analysis results of studied vehicle give bouncing, pitching and rolling modes. Natural frequencies of the studied vehicle are presented in Table 5. Amongst many natural frequencies and mode shapes, only first five modes represent in this paper those are influence much in dynamic responses of the structure. Figure 5 shows typical mode shapes and natural frequencies of 400m radius of curvature with 3% super-elevation of the studied bridge. Curvature plays an important role of the natural frequencies, whose vertical mode tends to decrease, whereas torsional mode increases with the increase of curvature and combine torsional horizontal mode has same tendency to vertical mode as shown in Fig.6. Mode shapes are coupled with bending and torsional vibrations and its effect is large with increasing curvature. In vertical modes, two main girders are vibrative in the same directions and the magnitude of the outside main girder vibration is always larger than that of the inside one and vice versa in the torsional modes. Also, the frequency ratio, which is the ratio of the first torsional and vertical mode frequencies, changes inversely with the radius of bridges. It can be observed that the frequency ratios of almost all studied models are small. Therefore, the torsional and vertical vibrations of these bridges could occur coincidently by external loads. So, it is practical to increase these values by improving torsional stiffness of studied bridges.

In case of providing different percentages of super-elevation first vertical mode is unpredictable, whereas first torsional mode tends to decrease for tight radius of curvature and second vertical mode tends to decrease with the increase of super-elevation shown in Table 6 and Fig.7. Providing super-elevation by creating hunch of the curved bridge, will contribute a slightly additional mass to the bridge. For that reason frequencies decrease slightly by increasing super-elevation.

3.2 Forced vibration analysis

In the present study, lumped mass system and Rayleigh damping[19] are assumed. Based on the experimental results of the approximately same bridges[20,21], one percent of critical damping is assumed for the first and second modes in most of the analyses. The friction between the truck tire and the bridge surface is mainly dependent upon the type of bridge pavement, the type of vehicle tire and the vehicle speed. The maximum lateral friction influences significantly the driver's comfort and allowable vehicle speed, but discomfort for passenger. In this study maximum friction coefficient of 0.18 is considered for all cases, that was also used Samaan et. al.[6]. The Newmark beta and Newton-Raphson procedures are selected to solve the problem. To get the initial conditions of the vehicle when entering into the bridge, the vehicle is run on an approach road of 45m long with the same road surface roughness. In each class of road surface, several correlated roughness profiles are analyzed to get the mean values of the dynamic responses. The dynamic load effect is measured in terms of maximum deflection throughout this study.

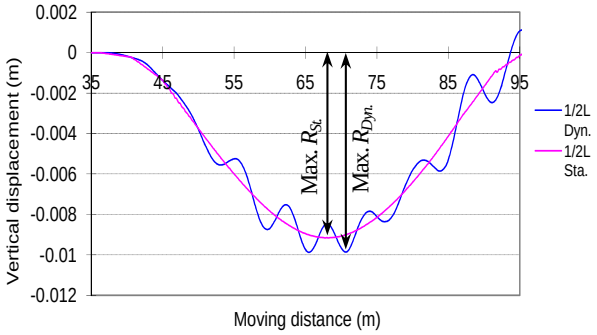


Fig.8 Mid-span deflection history

The Dynamic Amplification Factor (DAF) is defined as in equation (2).

$$DAF(\%) = \left(\frac{R_{Dyn.} - R_{Sta.}}{R_{Sta.}} \right) \times 100\% \qquad (2)$$

In which, $R_{Dyn.}$ and $R_{Sta.}$ are the absolute maximum responses of dynamic and static, respectively as shown in Fig.8. This is the deflection histories of dynamic and static of 400m radius curved bridge right girder at mid-span subjected to asymmetric lane position, vehicle moving at 60km/h on good road surface.

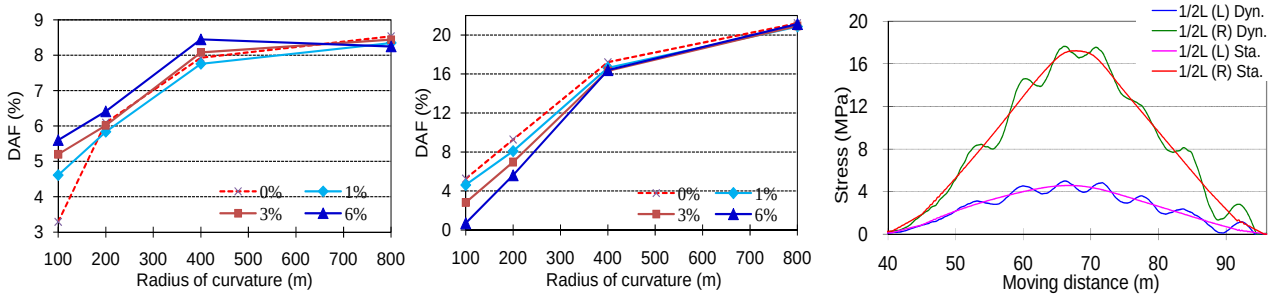
(1) Curvature and super-elevation effect

Dynamic amplification factors vary with radius of curvature and different percentages of super-elevation. The results given in Fig.9 are obtained for vehicle moving on outside lane under the velocity of 60km/h on good road surface roughness. Results shows DAFs are increasing with increasing radius of curvature. But increasing rate of inside and outside girder is different. Outside girder DAFs are smaller than those of inside girder. This could be attributed because, the higher the static response generated, the smaller the DAF is obtained as in equation (2). Bottom flange stresses at mid span of 200m radius of bridge with 3% super-elevation are shown in Fig.9c. This figure shows inside girder stress is smaller than that of outside girder. But inside girder vibration frequency is larger than that of outside girder due to the effect of curvature.

Super-elevation plays a role on DAFs as shown in Fig.9a,b. Three different percentages of super-elevation and another model without super-elevation are investigated to clarify the effect of super-elevation. DAFs of inside girder tend to decrease and for outside girder DAFs increase with increasing super-elevation due to vertical force distribution of vehicle and torsional effect. It is also found that, for tight radius of curvature super-elevation effect is large. But in 800m radius of curvature the variations of DAFs are undistinguishable, which is almost straight bridge.

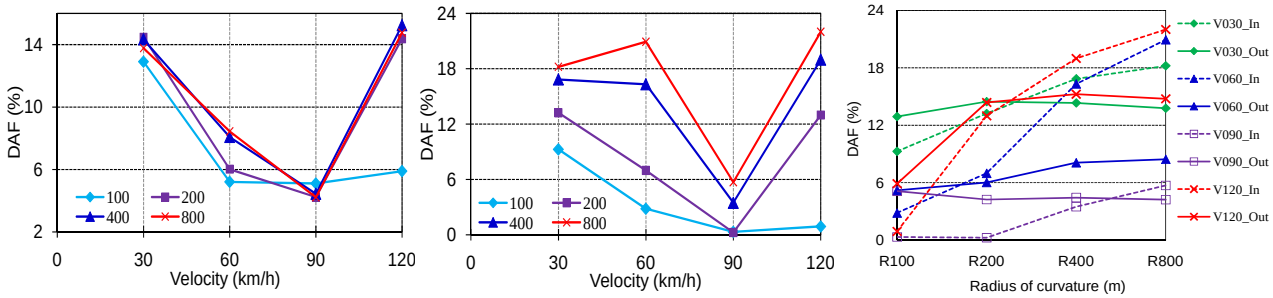
(2) Vehicle speed effect

Figure 10 gives the variations of dynamic amplification factors of outside and inside girders with various vehicle speeds for different radii of bridges based on the outside lane loading with good roughness condition and 3% super-elevation. It can be seen from the figure that the DAFs are fluctuates with the increase of vehicle speed. In the range of studied speeds, it seems



a) Outside girder **b)** Inside girder **c)** Bottom flange stress at mid span

Fig.9 Effect of radius of curvature and super-elevation on DAF



a) Outside girder **b)** Inside girder **c)** DAF verses radius

Fig.10 Effect of vehicle speeds on DAF

to achieve its maximum values at the fastest and lowest speeds. However, in 90km/h vehicle speed, DAFs are lowest in all the cases. Because in this velocity low frequency dynamic responses occurs due to surface roughness, also contributing torsional mode as shown in Fig.11. Also in inside girder DAFs are larger than outside girder because static responses are higher in outside girder due to vehicle moving on outside lane. But, in 100m radius of curvature outside girder DAFs are larger than inside girder in every studied speed shown in Fig.10c. This is simply due to torsional effect of small radius of curvature. However in larger radius of bridge, big difference of the DAFs between two girders is observed.

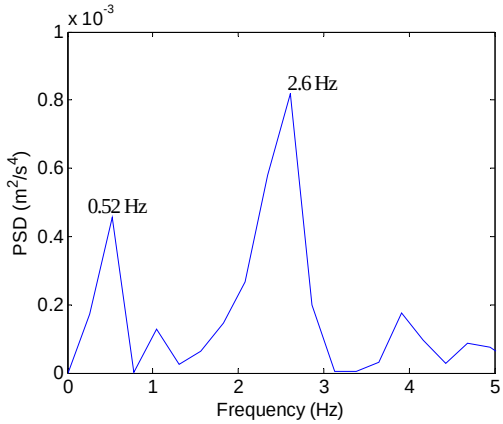


Fig.11 PSD for 90km/h of 200m radius bridge

(3) Loading position effect

In order to know the influence of the transverse loading position on the dynamic response of curved twin I-girder bridges, five loading positions are investigated as shown in Fig.12. The studied bridge was designed for two symmetrical traffic lanes separated by the centre line of bridge deck. In Loading 1 and Loading 2 cases, vehicle is run on the outside lane; only the difference is distance between the centerline of bridge and the centre of vehicle. In Loading 3 case, vehicle is run symmetrically on the centre of the bridge deck. In Loading 4 and Loading 5 cases, vehicle is run on the inside lane and the distance between the centerline of bridge and the centre of vehicle are the same of Loading 2 and Loading 1 respectively, but opposite direction from centerline of bridge. Four different radii of bridges with 3% super-elevation and good road surface roughness are considered of every analysis. In good road roughness class, several profiles are considered to get the mean values of dynamic amplification factors. According to previous section studies 30km/h and

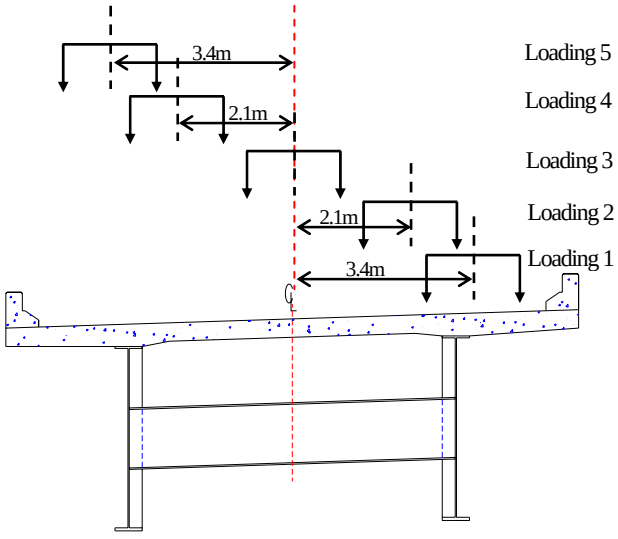
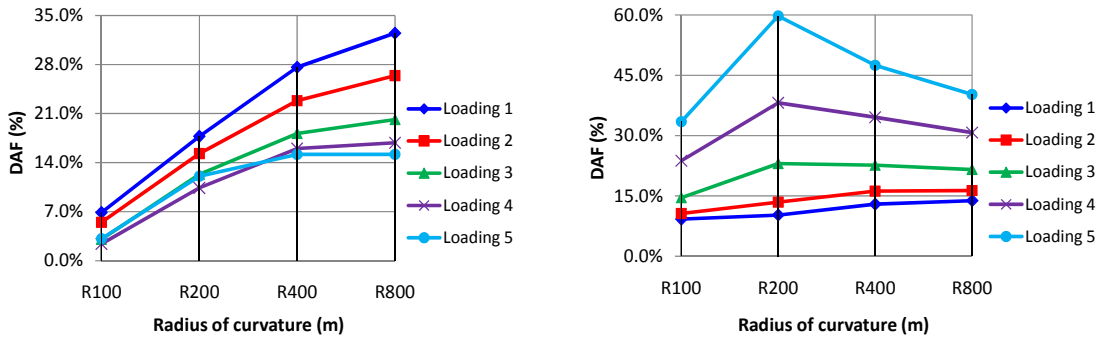
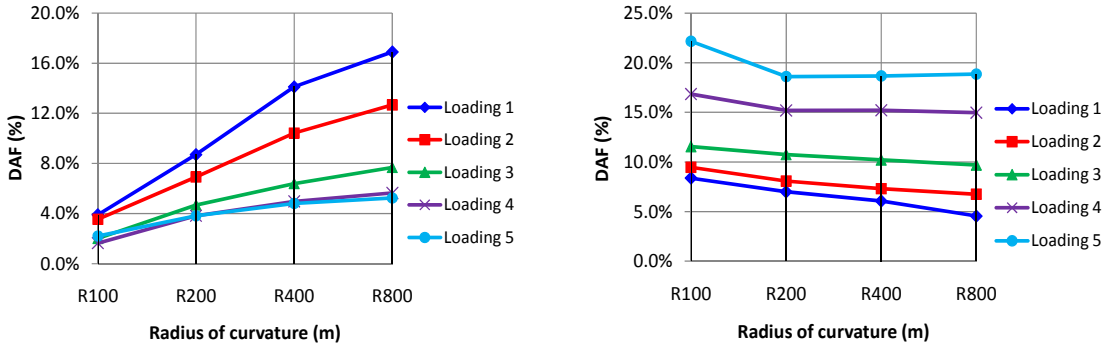


Fig.12 Vehicle loading model



a) Inside girder **b)** Outside girder

Fig.13 Influence of loading position for 30km/h vehicle speed



a) Inside girder **b)** Outside girder

Fig.14 Influence of loading position for 90km/h vehicle speed

90km/h vehicle speeds are affected a lot on DAF; that is why these speeds are chosen to study the effect of loading positions.

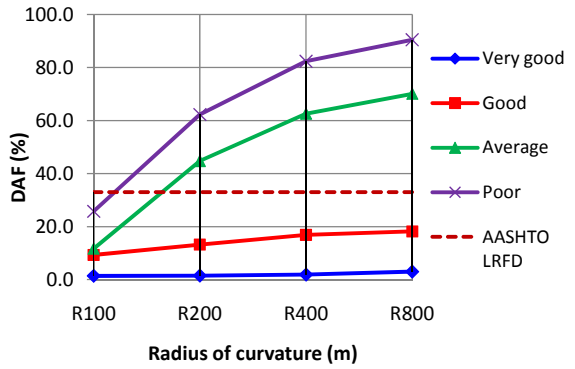
Loading positions effect for 30km/h and 90km/h vehicle speeds are shown in Fig.13 and Fig.14. It can be observed from the figures that the loading positions have a tremendous influence on the impact factor of each main girder. This could be attributed to the change of both static responses and torsional effects caused by different loading positions. Dynamic amplification factors of the inside girder decrease and those of outside girder increase, as the loading moves from outside to inside girder of every radii of bridges and both vehicle speeds. This could be due to increasing the wheel load distribution of the inside girder, that is, the larger the static responses generate, the smaller the DAF will be. Response behavior of two girders is different of different radius of curvature and both vehicle speeds. Inside girder DAFs decrease with increasing curvature of both vehicle speeds. But, in outside girder of small radius of curvature DAFs are fluctuating of every loading positions and both vehicle speeds due to torsional effect. Also 30km/h vehicle velocity produced higher DAFs of both girders than the 90km/h vehicle speed of every loading position.

(4) Roughness effect

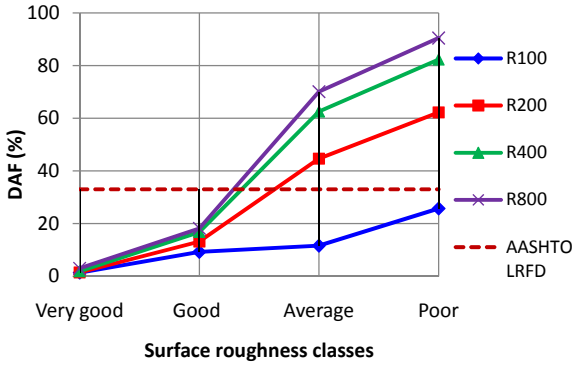
Road surface roughness plays an important role in the dynamic response of bridge-vehicle interaction system. Four roughness classes, namely very good, good, average and poor along with different vehicle speeds and different radius of curvature are analyzed to clarify its effect. Outside lane loading and 3% super-elevation are considered of every analysis.

Figure 15 illustrates the variation of the dynamic amplification factors of the inside girder with varying road surface classes, radius of curvature and vehicle speeds. Regardless the road surface classes, the DAFs vary with different radius of curvature and different vehicle speeds. It can be seen from the figures that DAFs are increasing with increasing radius of curvature. However, the small radius of curvature gives the small DAF in every roughness classes due to torsional effect. It is also found that, with the increasing of road surface roughness, the DAFs at all the cases increase distinctly. Dynamic amplification factors are maximum at the fastest studied speed of 120km/h and second highest value at the lowest studied speed 30km/h. However, very high value of approximately 220% DAF can be found when vehicle running at the fastest studied speed on the worst surface condition shown in Fig.15c. Because of worse the road surface is, the higher the DAFs will occur.

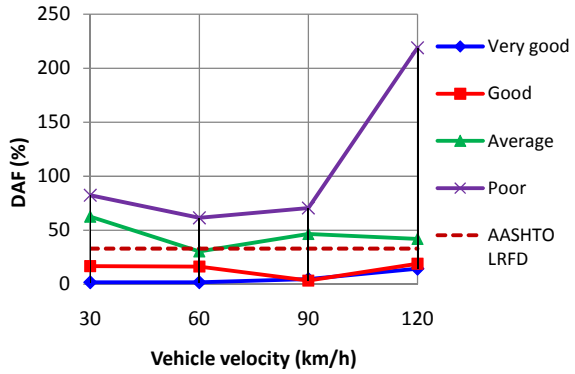
Calculated results are also compared with the value specified in AASHTO LRFD 2004 specifications[12]. Outside girder DAFs are well below the AASHTO specification value of very good, good and average road surface. Because outside lane loads generate larger static response of outside girder. But, in inside girder with very good and good road surfaces, the DAFs are well below the value given by AASHTO specifications as shown in Fig.15. For very small radii of bridge, DAFs of every roughness



a) DAF with radius of curvature

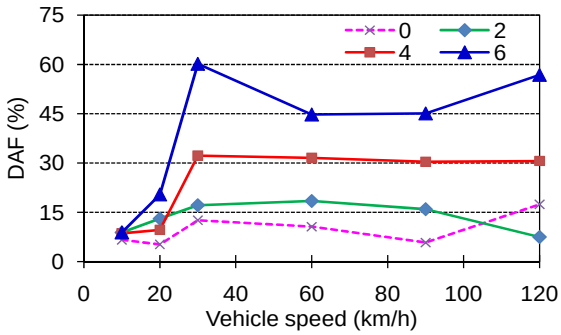


b) DAF with roughness classes

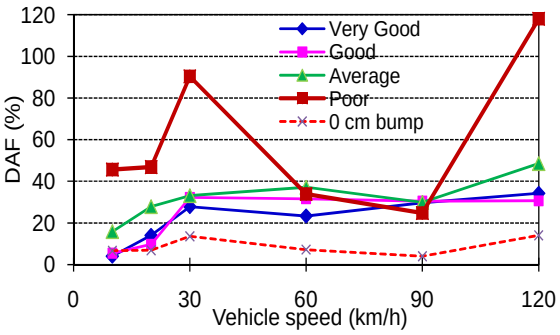


c) DAF with vehicle speed

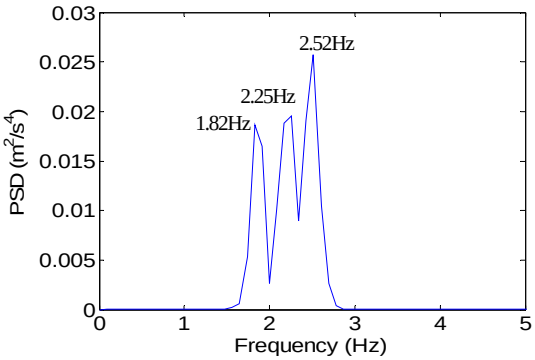
Fig.15 Surface roughness effects on DAFs



a) For good roughness class



b) Different roughness classes at 4cm bump height



c) PSD for 30km/h with 4cm bump height

Fig.16 Effect of bump height on DAF

classes are well below the value given by specifications. But, other radii of bridges with average and poor surfaces, the AASHTO LRFD specified value seems to underestimates of the dynamic amplification factor. These could be happen due to static response and torsional effect of curved bridge. Therefore, torsional stiffness increasing is necessary for curved bridges.

(5) Effect of bumps at expansion joint

Bump related problems have been commonly recognized and its causes are identified. But, no unified engineering solutions have emerged, primarily because of complexity. This section tries to establish correlations of bump heights, vehicle speeds, and roughness with dynamic amplification factors of the studied bridge. Three different bump heights (namely h = 2, 4 and 6cm) are considered for parametric study and another model without bump are investigated to clarify the effect of bumps. The studied bridge is considered 400m radius with 1% super-elevation and vehicle is run on the right side of the bridge deck. Dynamic amplification factors at mid-span of outside girder for good road roughness under various vehicle speeds and expansion bump heights are shown in Fig.16a.

It shows dynamic amplification factors changing with vehicle speeds and bump heights. As expected, the slowest studied speed of 10km/h has very little effect on the dynamic response of bridge. However, the highest speed of 120km/h does not cause the most unfavorable effect on the dynamic response of the bridge. The dynamic responses increase sharply and achieve their maximum values when vehicle running at 30km/h and then decrease quickly when increasing vehicle speed to 60km/h of every bump height. Dynamic responses are increased 45%, 45% and 57% with higher bump heights when vehicle running at higher speeds of 60, 90 and 120km/h respectively. DAFs are larger at 30km/h vehicle speed than others speed of every bump heights. Because

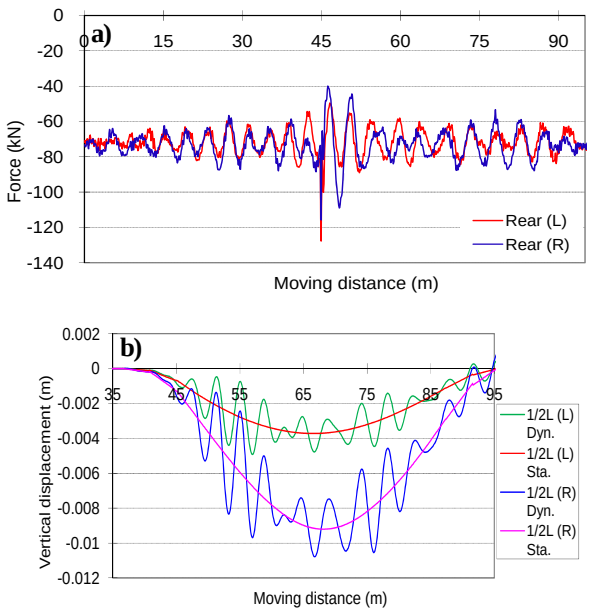


Fig.17 Bridge-vehicle interaction history (a) Vehicle rear tires force (b) Mid-span deflection of bridge

in this case dynamic response is dominated by combine effect of vehicle second mode (pitching) and first vertical mode of the bridge shown in Fig.16c. Others surface roughness results on the effect of bump give the same tendency but different DAF obtained of different roughness condition. Of course the poor roughness condition has higher DAF value and very good roughness has lower DAF value shown in Fig.16b. Force history of vehicle rear tires is shown in Fig.17a. When vehicle passing the expansion bump at that time maximum vehicle force is generated. Bridge dynamic responses reach their largest values when vehicle's position is somewhere at quarter span length, instead of mid span length as usual shown in Fig.17b. This could be attributed to vehicle large response right after passing the bump.

4. CONCLUSIONS

A three dimensional finite-element interaction analysis of horizontally curved twin I-girder bridges was conducted parametrically. Based on the results of the natural vibration and forced vibration analyses carried out in parametric study, the following remarkable conclusions can be made:

(1) Curvature plays an important role of the natural frequencies of curved I-girder bridges, whose vertical mode tends to decrease, whereas torsional mode increases with the increase of curvature. Mode shapes are coupled with bending and torsion and its effect is large with increasing curvature. Also, the frequency ratios of all studied models are small and need to increase this value by improving torsional stiffness.

(2) Super-elevation effect on natural frequency is small. However, first torsional mode frequency tends to decrease for tight radius of curvature and second vertical mode tends to decrease with the increase of super-elevation.

(3) The dynamic amplification factor of the girder which is directly under vehicle wheels seems smaller than that of remaining one, because the higher the static response generate, the smaller the DAF is obtained. The DAFs are increasing with increasing bridge radius. Super-elevation effects for small radius of curvature seem to have dramatic effect on DAF. DAF of inside girder decreases and of outside girder increases with increasing super-elevation due to vertical force distribution of vehicle and torsional effect.

(4) In the range of studied speeds, DAF seems to achieve its maximum value at the fastest and lowest speeds. The larger radius of bridges, the bigger the difference of the DAFs between two girders is observed.

(5) From the analysis of transverse loading positions, it could be seen that the larger the static response carried by a girder, the smaller the DAF will be. An appropriate loading position should be selected which can generate the maximum static response of girders to evaluate DAF. Otherwise, misrepresentation of DAF will occur in practical design of bridges.

(6) Road surface roughness is another important factor of the dynamic behavior of curved I-girder bridges. The worse the road surface is, the higher the DAF will occur. However, the small radius of curvature gives the small DAF in every roughness classes. In average and poor road surfaces, the AASHTO LRFD specified value seems to underestimates of DAF due to static response and torsional effect.

(7) The defects at expansion joint greatly impact on the dynamic response of the studied bridge. Higher the expansion bumps height, larger the DAF is obtained at same vehicle speed. At 30km/h, DAF is larger, because in this case dynamic response is dominated by combine effect of vehicle mode and first vertical mode of the bridge. Therefore, it is important to take into account this effect in practical design.

References

1) Linzell, D. G., Hall, D., and White, D., Historical perspective on horizontally curved I girder bridge design in the United States, *Journal of Bridge Engineering*, Vol. 9, No. 3, pp.218-229, 2004.
2) Senthilvasan, J., Thambiratnam, D. P. and Brameld, G. H., Dynamic response of a curved bridge under moving truck load, *Engineering Structures*, Vol. 24, pp.1283-1293, 2002.
3) Sennah, K. and Kennedy, J. B., Vibrations of horizontally curved continuous composite cellular bridges, *Canadian Journal of Civil Engineering*, Vol. 25, pp.139-150, 1998.
4) Huang, D., Wang, T. L. and Shahawy, M., Dynamic behavior of horizontally curved I-girder bridges, *Computer & Structures*, Vol. 57, No. 4, pp.703-714, 1995.
5) Huang, D., Wang, T. L. and Shahawy, M., Vibration of horizontally curved box girder bridges due to

vehicle, *Computer & Structures*, Vol. 68, pp. 513-528, 1998.
6) Samaan, M., Kennedy, J. B. and Sennah, K., Impact factors for curved continuous composite multiple-box girder bridges, *Journal of Bridge Engineering*, Vol. 12, No. 1, pp.80-88, 2007.
7) Genin, J., Ting, E. C. and Vafa, Z., Curved bridge response to a moving vehicle, *Journal of Sound and Vibration* , Vol. 81, No. 4, pp.469-475, 1982.
8) Mermertas, V., Dynamic interaction between the vehicle and simple supported curved bridge deck, *Computer Methods in Applied Mechanics and Engineering*, Vol. 162, pp.125-131, 1998.
9) Kwasniewski, L., Li, H., Wekezer, J. and Malachowski, J., Finite element analysis of vehicle-bridge interaction, *Finite Elements in Analysis and Design*, Vol. 42, pp.950-959, 2006.
10) Martin, T. M., Barton, F. W., McKeel, W. T. and Gomez, J. P., Effect of design parameters on the dynamic response of bridges, *Final report-Virginia Transport Research Council*, Virginia, USA, 2000.
11) Design Quality Assurance Bureau NYSDOT, *Recommendations for AASHTO Super-elevation Design*, September, 2003.
12) The American Association of State Highway and Transportation Officials, *AASHTO LRFD Bridge Design Specifications*, 2004.
13) Ngo-Tran, T. L., Hayashikawa, T. and Matsumoto, T., Three-dimensional bridge-vehicle interaction analysis of simply supported twin I-girder bridge, *Journal of Structural Engineering*, Vol. 54A, pp. 181-188, 2008.
14) Wang, T. L. and Huang, D., Computer modeling analysis in bridge evaluation, *Final report – Highway Planning and Research Program*, Miami, Florida, 1992.
15) Dodds, C. J. and Robson, J. D., The description of road surface roughness, *Journal of Sound and Vibration*, Vol. 31, No. 2, pp.175-183, 1973.
16) Honda, H. Kajikawa, Y. and Kobori, T., Spectra of road surface roughness on bridges, *Journal of the Structural Division (ASCE)*, Vol. 108 (ST9), pp. 1956-1966, 1982.
17) Sayers, M. W., Dynamic terrain inputs to predict structural integrity of ground vehicles, *Technical report – Transportation Research Institute*. The University of Michigan, 1988.
18) Simo J. C. and Laursen T. A., An augmented Lagrangian treatment of contact problems involving friction, *Computers & Structures*, Vol. 42, No. 1, pp.97-116, 1990.
19) Clough, R. W. and Penzien, J., *Dynamics of Structures*, McGraw-Hill Book Co., Second Edition, 1993.
20) Kim, C. W., Kawatani, M., and Hwang, W. S., Reduction of traffic-induced vibration of two-girder steel bridge steated on elastomeric bearings, *Engineering Structures*, Vol. 26, pp.2185-2195, 2004.
21) Huang, D., Wang, T. L., and Shahawy, M., Impact analysis of continuous multigirder bridges due to moving vehicles, *Journal of Structural Engineering*, Vol. 118, No. 12, pp.3427-3443, 1992.

(Received September 16, 2010)